THE PROTEIN SOCIETY

METHODS AND APPLICATIONS

Kinetic analysis of cytokine-mediated receptor assembly using engineered FC heterodimers

Ashlesha Deshpande, Balananda-Dhurjati Kumar Putcha, Srilalitha Kuruganti, and Mark R. Walter *

Department of Microbiology, University of Alabama at Birmingham, Birmingham, Alabama, 35294

Received 7 March 2013; Accepted 14 May 2013
DOI: 10.1002/pro.2285
Published online 23 May 2013 proteinscience.org

Abstract: A method for analyzing ligand–receptor binding kinetics is described, which is based on an engineered FC domain (FChk) that forms a covalent heterodimer. To validate the system, the type I IFN receptors (IFNAR1 and IFNAR2) were expressed as IFNAR1-FChk, IFNAR2-FCkh, and IFNAR1/IFNAR2-FChk fusion proteins. Surface plasmon resonance (SPR) analysis of binary IFNα2a/IFNAR interactions confirmed prior affinity measurements, while the affinity of the IFNα2a/IFNAR1/IFNAR2-FChk interaction reproduced the affinity of IFNα2a binding to living cells. In cellular assays, IFNAR1/IFNAR2-FChk potently neutralized IFNα2a bioactivity with an inhibitory concentration equivalent to the K_D measured by SPR. These studies suggest that FChk provides a simple reagent to evaluate the binding kinetics of multiple ligand–receptor signaling systems that control cell growth, development, and immunity. © 2013 The Protein Society

Keywords: surface plasmon resonance; engineered FC; cytokine; interferon; IFNAR1; IFNAR2; heterodimer

Introduction

Cytokines transmit signals across the cell membrane by oligomerizing cell surface receptors.[1–4] Crystal structure analysis has shown that the basic signaling unit is often a ternary complex, where the cytokine assembles either two identical receptors (homodimerization), or two different receptors (heterodimerization), to activate cellular activity.[1,5–8] In either case, one receptor chain usually exhibits enhanced affinity to capture ligand to the cell surface, whereas the second chain recognizes this binary complex to form the functional ternary signaling complex. The tuning of receptor–ligand affinities is important not only for regulating the strength of signal through the membrane but also to

Conflict of interest: A patent has been filed on the reagents and methods described in this proposal

Ashlesha Deshpande and Balananda-Dhurjati Kumar Putcha contributed equally to this work

Grant sponsor: NIH; Grant numbers: 1R01-AI047300, AI0473-S1, R21-AI081065, 5R01AI097629. Grant sponsor: Lupus Research Institute.

*Correspondence to: Mark R. Walter, Department of Microbiology, The University of Alabama at Birmingham, 1025 18th Street South, Birmingham, AL 35294, USA. E-mail: walter@uab.edu

control targeting of cytokines to specific cells. The direct link between receptor binding and biological function emphasizes the need to accurately measure these protein–protein interactions to improve our understanding of cell communication and facilitate the development of improved cytokine biologics.

The analysis of monomeric ligand–receptor binding kinetics is routinely performed using surface plasmon resonance (SPR). However, cytokine binding to receptor heterodimers, the actual functional units required for signaling, is usually not evaluated. A major reason for this is the three-dimensional nature of biacore chip dextran layers, which do not mimic the planar lipid environment of the cell membrane. To overcome this problem, coiled-coil domains have been used to assemble receptor heterodimers.[9,10] This eliminates the problem of chip surface heterogeneity by placing the receptors adjacent to one another. However, purification and coupling of the molecules to the chip surface are often problematic. Elegant studies have recently been performed on supported lipid bilayers by attaching histidine-tagged receptors to bis-NTA-coupled lipids that allow the receptors to undergo lateral movement.[11,12] However, these studies require considerable expertise to perform and do not seem appropriate for general laboratory use.

Immunoglobulin FC domains are often used in biotechnology and therapeutic applications. Several cell surface receptors (e.g., CLTA-4, IL-1R, LFA-3, and TNFR) fused to FC domains have been approved as human therapeutics.[13] Ridgway *et al*. have extended the utility of the FC by identifying steric "knobs into holes" (kh) mutations in the CH3–CH3 dimer interface that promote formation of an FC heterodimer (FCkh) that allows the production of bispecific Abs.[14] However, the cysteines in the Ab hinge region of the Abs form disulfide bonds regardless of whether FC dimers (e.g., two FCk or two FCh chains), or heterodimers (e.g., an FCk and FCh chain), are assembled.

To generate an improved reagent for the analysis of cytokine-receptor monomer and heterodimer interactions by SPR, the "symmetric" Ab hinge region of FCkh has been replaced with cysteine residues engineered to form a disulfide bond specific for FCkh heterodimer formation. This design has resulted in an improved FCkh reagent that functions as a purification tag, coupling reagent, and heterodimerization domain that allows analysis of monomeric and heterodimeric ligand–receptor interactions. To test the system, the type I IFN receptors, IFNAR1 and IFNAR2, were produced as IFNAR-FChk fusion proteins for SPR analysis (Fig. 1). Type I interferons (IFNs) induce antiviral, antiproliferative, and immunomodulatory activities on diverse cell types.[15–17] Several studies have shown that receptor binding affinity is directly related to the biological activity of the IFNs.[18–20] In addition,

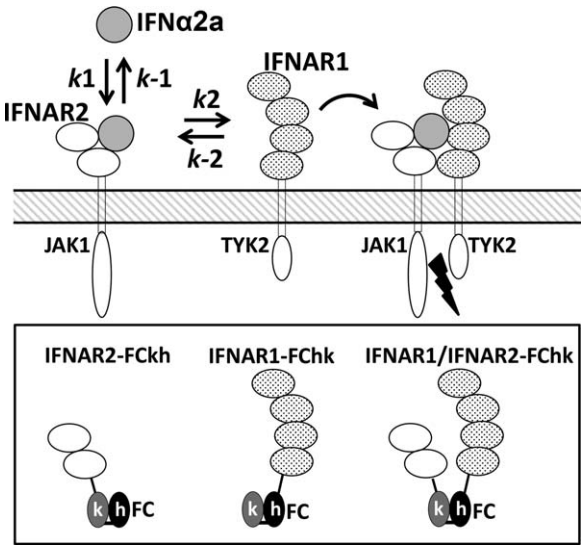

Figure 1. Schematic diagram of IFNα2a receptor assembly and IFNAR-FChk molecules used for SPR analysis.

biophysical studies have characterized IFN/IFNAR receptor interactions using diverse methods.[21,22] For these reasons, the type I IFN receptor system was used to test the functionality of FChk to assemble, purify, and characterize IFN binding kinetics to monomeric and heterodimeric IFNARs. SPR analysis demonstrated that the affinity of the IFNα2a/IFNAR1/IFNAR2-FChk interaction was equivalent to the affinity of IFNα2a binding to living cells.[18] These studies confirm the usefulness of this simple system for studying a wide variety of diverse protein–protein interactions with affinities that span over five orders of magnitude.

Results

Design and production of a disulfide-linked FCkh heterodimer

A FC heterodimer (FCkh) was designed based on a previously described "knob-into-holes" strategy[14] by inserting knob (k, T366Y) and hole (h, Y407T) mutations into separate plasmids (FCh and FCk) encoding an antibody IgG2a heavy-chain FC region. Using the IgG2a crystal structure (PDB ID = 1IGT[23]), cysteine residues were positioned into FCk and FCh to selectively form an interchain disulfide bond upon FCkh heterodimer formation. To accomplish this, the FC dimer interface was interrogated for inter-interface amino acid positions (within ~8 Å of one another) that would allow disulfide bond formation upon heterodimer formation, but not upon FC homodimerization. Based on this analysis, an E376C mutation was added to the FCk chain and a "GGCGT" sequence was encoded at the C-terminus of FCh, following residue F472.

Coexpression of FCk and FCh chains efficiently formed (~100%) disulfide-linked FCkh heterodimers

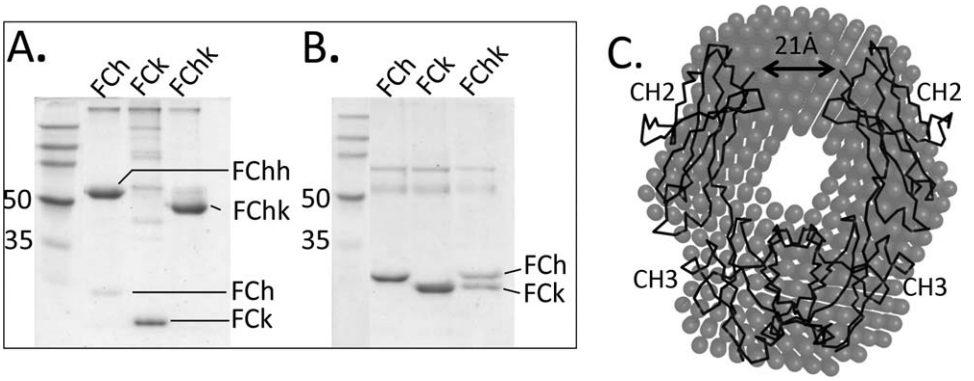

Figure 2. Analysis of FCh/FCk assembly and structure. Labels at the top of the gels denote transient expression of plasmids encoding FCh, FCk, and FCh + FCk (labeled FChk) in insect cells. The ability of the proteins to assemble into disulfide-linked homodimer or heterodimer was evaluated by SDS-PAGE under oxidizing (A) and reducing (B) conditions. DAMAVER bead model (grey) of FChk derived from the SAXS data (C). An alpha carbon representation of the FC domain (black) from 1IGT is shown fit into the average bead model. The arrow points to residue G250 in the CH2 domains and the distance between these residues.

rather than FCkk and FChh homodimers (Fig. 2). FCk expressed alone does not assemble into disulfide-linked FCkk dimers, whereas expression of FCh efficiently forms disulfide-linked FChh homodimers. The solution structure of FCkh was determined by small-angle X-ray scattering (SAXS) to confirm that FChk adopts the same overall structure as the FC crystal structure (1IGT). Radius of gyration (R_g) and d_{max} values obtained from the SAXS data (R_g = 28.8 Å, d_{max} = 75 Å) were similar to values calculated for the FC crystal structure (R_g = 25.5 Å, d_{max} = 82.5). The fit of the FC crystal structure into the average bead model suggests that the N-termini of the CH2 domains in FCkh are separated by ~21 Å [Fig. 2(C)]. This distance is approximately twice as large as observed for the N-termini of heterodimeric coiled-coil assembly domains.[24,25]

Production and ligand-binding properties of IFNAR1-FChk and IFNAR2-FCkh monomers

To determine if FCkh could be used to purify and attach receptors to biacore chips for SPR experiments, the extracellular regions of IFNAR1 and IFNAR2 were cloned in frame with FCh and FCk, respectively. To assemble IFNAR1-FChk and IFNAR2-FCkh fusion proteins (Fig. 1), plasmids encoding IFNAR1-FCh and FCk, as well as IFNAR2-FCk and FCh, were coexpressed in insect cells. IFNAR1-FChk and IFNAR2-FCkh were purified from the expression media by protein A and size exclusion chromatography [SEC, Fig. 3(A)]. On the size exclusion column, IFNAR1-FChk and IFNAR2-FChk ran at molecular weights (MWs) of 122 and 82 kDa, respectively [Fig. 3(A)]. FChk disulfide bond formation was confirmed by SDS-PAGE analysis of

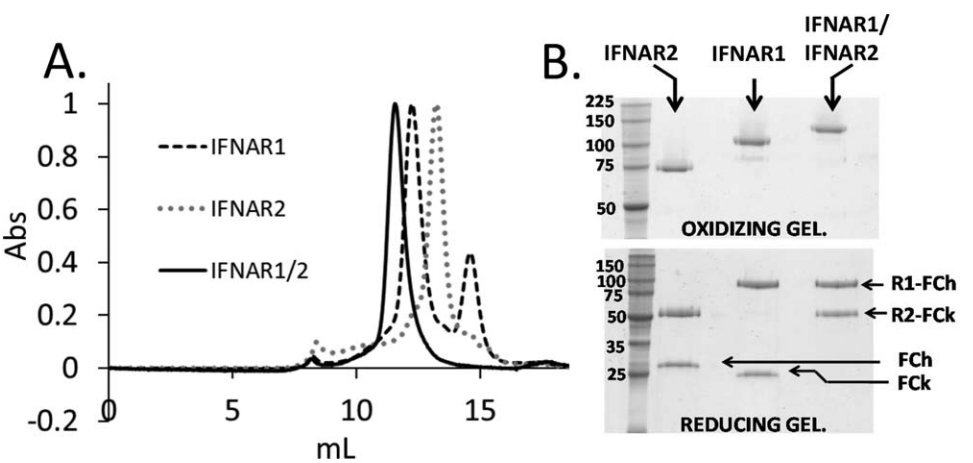

Figure 3. Characterization of IFNAR-FC fusion proteins. (A) Size exclusion chromatographs of IFNAR1-FChk (dashed line), IFNAR2-FChk (grey dots), and IFNAR1/IFNAR2-FChk (black line). SDS-PAGE analysis of the purified fusion proteins under oxidizing (top gel) and reducing (bottom gel) conditions (B). For clarity, the FC designations are not added to the chromatographs or to labels across the top of the gel.

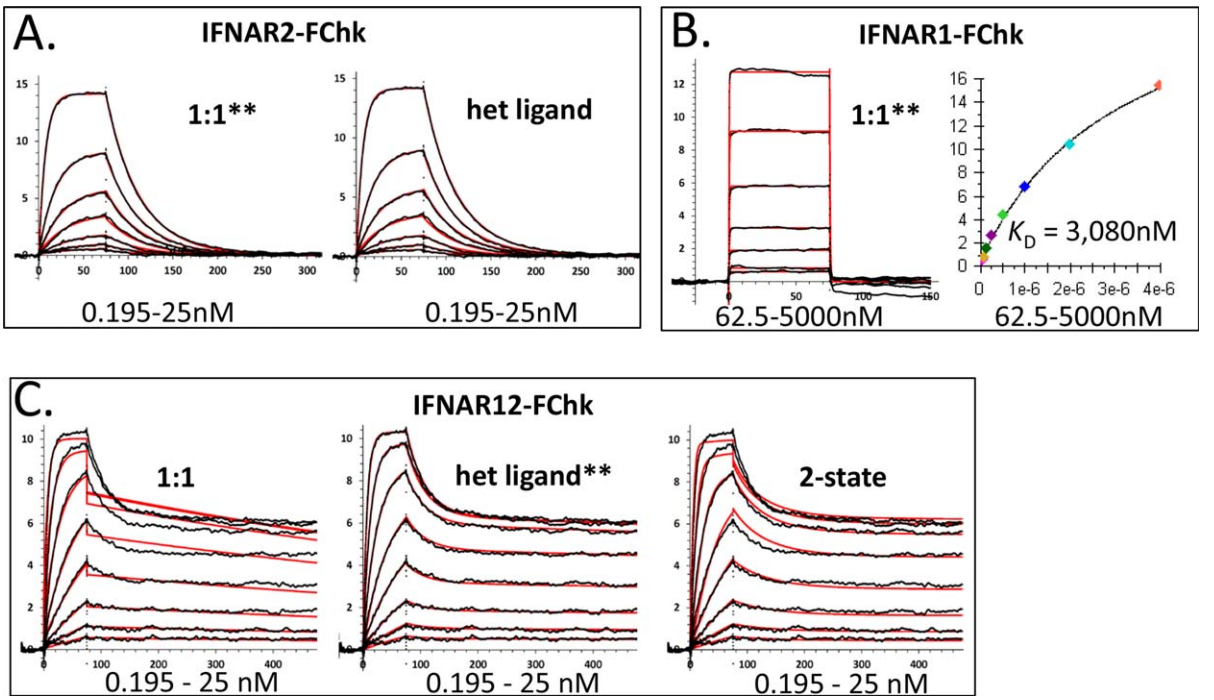

Figure 4. IFNα2a binding to IFNAR-FC fusion proteins. SPR sensorgrams (black) are shown for IFNα2a binding to IFNAR2-FCkh (A), IFNAR1-FChk (B), and the IFNAR1/IFNAR2-FChk heterodimer (C). The model used to fit each sensorgram is denoted in the figure along with the resulting fit (red lines) to the data. The selected model discussed in the text is denoted by **. Sensorgrams were collected by injecting twofold dilutions of IFNα2a over the concentrations shown on each figure. Kinetic constants for the SPR experiments are shown in Tables I and II. The equilibrium dissociation constant (K_D) for the IFNα2a/IFNAR1 interaction is also shown in (B). [Color figure can be viewed in the online issue, which is available at wileyonlinelibrary.com.]

IFNAR1-FChk and IFNAR2-FCkh under oxidizing and reducing conditions [Fig. 3(B)]. Under oxidizing conditions the fusion proteins ran as single bands with MWs observed by SEC. However, on reducing gels, the proteins separated into two bands corresponding to IFNAR1-FCh and FCk, or IFNAR2-FCk and FCh [Fig. 3(B)]. This analysis confirmed that FCkh can be used to assemble monomeric IFNAR1-FCkh and IFNAR2-FCkh fusion proteins as opposed to commonly produced FC receptor dimers.

The IFNα2a/IFNAR2 interaction was studied by injecting IFNα2a over IFNAR2-FCkh, which was coupled to a biacore chip using an anti-FC antibody [Fig. 4(A)]. Sensorgrams from three experiments were fit to a 1:1 binding model resulting in k_a and k_d values of 5.5×10^6 $M^{-1}s^{-1}$ and 0.032 s^{-1}, which corresponds to an equilibrium dissociation constant (K_D) of 5.8 n*M* (Table I). The observed binding constants are consistent with previous values obtained for the IFNα2a/IFNAR2 interaction using different experimental methods.[21] IFNα2a was also injected (78–5000 n*M*) over IFNAR1-FChk coupled to biacore chip surfaces [Fig. 4(B)]. Three equilibrium experiments yielded a K_D of 3080 n*M* for the IFNα2a/IFNAR1-FChk interaction. A K_D value of 3692 n*M* was obtained from rate constants ($k_a = 6.5 \times 10^5$ $M^{-1}s^{-1}$ and $k_d = 2.4$ s^{-1}), determined from a single kinetic experiment. The K_D value obtained for the IFNα2a/IFNAR1-FChk interaction is also similar to previously reported values (K_D = 3–5 μ*M*).[22] Together, these studies validate the use of the FCkh heterodimers for SPR analysis of cytokine–receptor interactions.

Production and analysis of IFNAR1/IFNAR2-FChk heterodimers

To evaluate IFNα2a binding to IFNAR1 and IFNAR2, plasmids encoding IFNAR1-FCh and IFNAR2-FCk were coexpressed in insect cells to produce an IFNAR1/IFNAR2-FChk heterodimer (Fig. 1). Media from the expression experiment were purified by protein A chromatography and SEC [Fig. 3(A)]. The estimated MW of IFNAR1/IFNAR2-FChk on SEC is 160,300, which is consistent with its predicted MW of 137,405. The predicted MW includes 15,585 Da of N-linked carbohydrate, which corresponds to insect cell-derived hexasaccharides (1039 Da each) attached to each of the 15 predicted NXS/T-linked sites in the heterodimer.[26] SDS-PAGE analysis of IFNAR1/IFNAR2-FChk under oxidizing and reducing conditions confirmed that IFNAR1-FCh and IFNAR2-FCk chains are covalently linked by a disulfide bond [Fig. 3(B)]. Thus, the same MW and 1:1 stoichiometry of IFNAR1/IFNAR2-FChk, as well as IFNAR1-FChk and IFNAR2-FCkh, was confirmed by SEC and SDS-PAGE analysis.

Table I. *Binding Parameters for IFNα2a/IFNAR-FChk Interactions*

	$k_{1a} \times 10^5$ (M^{-1} s^{-1})	k_{1d} (s^{-1})	K_D (n*M*)	$k_{2a} \times 10^5$ (M^{-1} s^{-1})	$k_{2d} \times 10^{-4}$ (s^{-1})	K_D (p*M*)
IFNAR1-FChk[a]	6.5 ± 0.3	2.4 ± 0.1	3692	—	—	—
IFNAR2-FCkh[a]	55 ± 8	0.032 ± 0.003	5.82	—	—	—
IFNAR2-FCkh[b]	47 ± 0.2	0.036 ± 0.001	7.59	42.0 ± 0.1	210 ± 0.27	5100
IFNAR12-FChk[a]	62 ± 0.06	0.00073 ± 0.5e^{-5}	0.12	—	—	—
IFNAR12-FChk[b]	43 ± 1	0.031 ± 0.004	7.21	59.5 ± 0.1	1.52 ± 0.07	25.5
IFNAR1/IFNAR2 molar ratio[c]						
4.3	79 ± 1.0	0.042 ± 0.001	5.32	2.2 ± 0.1	2.4 ± 0.01	10,909
1.7	57.0 ± 0.3	0.034 ± 0.001	5.96	1.08 ± 0.01	4.3 ± 0.01	39,815
0.5	70.1 ± 0.8	0.049 ± 0.004	6.99	29.5 ± 0.1	5.1± 0.01	1729
0.0	37.3 ± 0.2	0.034 ± 0.002	9.00	37 ± 0.2	34.0± 2.0	9000

Each sensorgram was fit with a heterogeneous ligand model.
[a] Sensorgrams fit with 1:1 model.
[b] Sensorgrams fit with heterogeneous ligand model.
[c] Molar ratio of IFNAR1-FChk to IFNAR2-FCkh, where IFNAR2-FCkh was coupled at constant level of 40 RU.

SPR sensorgrams collected for IFNα2a binding to the IFNAR1/IFNAR2-FChk were complex, meaning that they could not be fit with a simple 1:1 binding model [Fig. 4(C)]. As IFNAR1/IFNAR2-FChk is an assembly of two receptors (IFNAR1 and IFNAR2), a heterogeneous ligand model (HLM) incorporating two distinct rate equations was used to fit the sensorgrams. IFNα2a/IFNAR1/IFNAR2-FChk sensorgrams fit with the HLM resulted in one binding constant equivalent to the IFNα2a/IFNAR2-FCkh binary complex (K_D = 7.2 n*M*), whereas the second K_D value (26 p*M*) approximated the K_D of IFNα2a binding to living cells and to IFNARs attached to supported lipid bilayers (Table I[18,22]. The HLM yielded the best agreement to the experimental sensorgrams, which is shown by comparing 1:1, HLM, and two-state model fits in Figure 4(C). The K_D derived from each model ranges from 120 p*M* (1:1 model, Table I) to 8 p*M* for the two-state model (Table II). The HLM and two-state models were also applied to the IFNα2a/IFNAR2-FCkh sensorgrams as a control [Fig. 4(B), Tables I and II]. These studies demonstrated that the HLM yielded essentially the same K_D and rate constants as observed for the 1:1 model [Fig. 4(B) and Table II]. The two-state model applied to the IFNα2a/IFNAR2-FCkh sensorgrams yielded the same K_D value (Table II) obtained using the 1:1 and HLM, with an additional set of rate constants that were not required for the fitting. Interestingly, the second off-rates (k_{2d}) in the two-state model were decreased by ~10-fold relative to off-rates obtained in the 1:1 and HLM. Overall, this suggests that the appropriate model for analysis of the IFNα2a/IFNAR1/IFNAR2-FChk sensorgrams is the HLM.

Use of the HLM suggests that IFNα2a forms a mixture of IFNα2a/IFNAR2 binary complexes and IFNα2a/IFNAR1/IFNAR2 ternary complexes on the chip surface. The chemical purity of IFNAR1/2-FChk (Fig. 3) suggests that the heterogeneous binding properties are not due to problems with the stoichiometry of the heterodimer. It is possible that a fraction of IFNAR1-FCh within the IFNAR1/IFNAR2-FChk heterodimer is unable to bind IFNα2a, owing to steric occlusion, upon attachment to the SPR chip surface, which prevents capture of IFNAR2/IFNα2a complexes by IFNAR1. The percent of IFNα2a/IFNAR1/IFNAR2-FChk ternary complexes formed, relative to IFNα2a/IFNAR2 binary complexes, was estimated to be 55% from analysis of RU_{max} values calculated in the HLM fitting routine. Good agreement was observed between the calculated RU_{max} values, derived from the HLM, and the RU_{max} value observed in the SPR sensorgrams. Specifically, the sum of the two calculated RU_{max} values was 5.3 and 6.5 RU (11.8 total), respectively, whereas the observed RU_{max} from the 25 n*M* IFNα2a sensorgram was 10.4 RU. To further validate the affinity of the IFNα2a/IFNAR1/IFNAR2-FChk interaction determined by SPR, the ability of IFNAR1/IFNAR2-FChk to neutralize IFNα2a-mediated gene induction was tested using cells stably transfected with a luciferase reporter under control of the IFN-inducible 6-16 gene promoter (Fig. 5).[27] The inhibitory concentrations (IC_{50}) of IFNAR1/IFNAR2-FChk required to block the activity of 8 p*M* or 5 n*M* IFNα2a were 25.5

Table II. *Two-State Binding Parameters for IFNα2a/IFNAR-FChk Interactions*

	$k_a \times 10^6$ (M^{-1} s^{-1})	k_d (s^{-1})	k_a (s^{-1})	k_d (s^{-1})	K_D (p*M*)
IFNAR2-FCkh[a]	4.7 ± 8	0.029 ± 0.003	0.00015 ± 0.4e^{-4}	0.0021 ±2.0e^{-4}	5850
IFNAR12-FChk[a]	14 ± 0.2	0.013 ± 0.001	0.0086 ± 1.0e^{-4}	0.000072 ± 3.0e^{-5}	8.0

[a] Sensorgrams fit with two-state model.

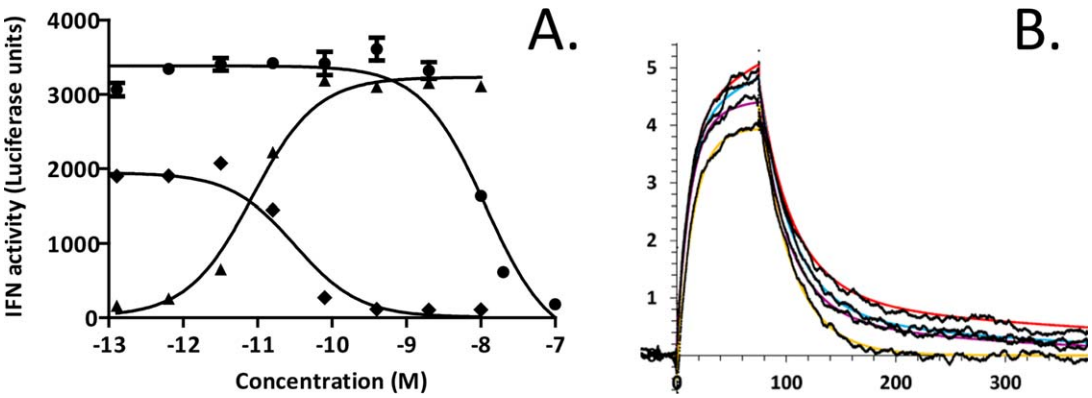

Figure 5. Luciferase assay (A) showing IFNα2a dose-response curve (triangles) and neutralization of constant IFNα2a (8 p*M*, diamonds; 5 n*M*, circles) with increasing IFNAR1/IFNAR2-FChk concentrations. Black lines correspond to nonlinear least square fits of the data using Sigma plot. (B) Sensorgrams (black) and model fits (different colored lines) for 10 n*M* injections of IFNα2a over biacore chips coupled with constant IFNAR2-FCkh (40RU) and IFNAR1-FChk levels of 0 RU (yellow line), 25 RU (purple line), 88 RU (cyan line), and 228 RU (red line). This corresponds to IFNAR1/IFNAR2 molar ratios of 0, 0.5, 1.7, and 4.3, respectively. Kinetic constants for the SPR experiments are shown in Table I. [Color figure can be viewed in the online issue, which is available at wileyonlinelibrary.com.]

p*M* and 11.6 n*M*, respectively. From these experiments, the IFNAR1/IFNAR2-FChk affinity constant (K_i) was estimated as 12.5–18.5 p*M* using the Cheng-Prusoff equation,[28] which is similar to the K_D value determined by SPR (Table I).

IFNAR1/IFNAR2-FChk was coupled at low levels to prevent mass transport, suggesting that the resulting K_D represents the inherent stability of the IFNα2a/IFNAR1/IFNAR2 ternary complex. The binding results obtained with IFNAR1/IFNAR2-FChk were compared against biacore chips coupled with monomeric IFNAR1-FChk and IFNAR2-FCkh in a similar manner to the studies first performed by Lamken *et al*. on supported lipid bilayers.[22] For these experiments, a constant level of IFNAR2-FCkh was captured (40 RU) on the chip with three different amounts of IFNAR1-FChk corresponding to IFNAR1/IFNAR2 molar ratios of 4.4:1, 1.6:1, and 1:0.5, respectively (Table I). For each surface, a sensorgram corresponding to a single injection of 10 n*M* IFNα2a was fit with the HLM [Fig. 5(B)]. As previously observed with IFNAR1/IFNAR2-FChk, one set of binding constants corresponded to the IFNα2a/IFNAR2 interaction. However, the K_D values for the second interaction ranged from 1.7 to 40 n*M*. The on-rate for the second interaction was $\sim 1 \times 10^5$ M^{-1} s^{-1}, which is similar to the on-rate observed for the IFNα2a/IFNAR1-FChk interaction (Table I). The off-rate of the second binding site was intermediate between the IFNα2/IFNAR1/IFNAR2-FChk and IFNα2/IFNAR2-FCkh interactions (~0.002–0.005 s^{-1}). The levels of IFNAR1-FChk and IFNAR2-FCkh coupled did not differ significantly from IFNAR1/IFNAR2-FChk (~100 RU). This suggests that the heterogeneous positioning of IFNAR1-FChk and IFNAR2-FCkh prevents efficient assembly of the IFNα2a/IFNAR1/IFNAR2 complex. However, the IFNα2a off-rate on the mixed surfaces is slower than for IFNAR2 alone, which may be caused by IFNα2a being shuttled between IFNAR1-FChk and IFNAR2-FCkh that are separated in space by distances greater than IFNAR1 and IFNAR2 attached to a single FChk domain.

Discussion

In this study, structure-based engineering was used to produce a disulfide-linked FChk domain to allow the characterization of cytokine binding to individual receptor chains and to signaling competent receptor heterodimers. As an example system, monomeric IFNAR1-FChk and IFNAR2-FCkh receptors, as well as IFNAR1/IFNAR2-FChk heterodimers were produced for binding studies. Because of the large body of biochemical and biological data, and the distinct MWs of the extracellular receptor chains (IFNAR1 ~50,000 and IFNAR2 ~25,000), the IFNAR receptor system was ideal to characterize the utility of FChk. SPR analysis of IFNα2a binding to IFNAR1/IFNAR2-FChk yielded a K_D of 26 p*M*, which is very similar to the affinity of IFNα2a binding to cells ($K_D \sim 26$ p*M*) and to IFNARs attached to supported lipid membranes.[18,22] This suggests that the IFNAR1/IFNAR2-FChk heterodimers can mimic some features of the membrane-bound receptor chains.

The high-affinity IFNα2a/IFNAR1/IFNAR2-FChk interaction could not be reproduced by coupling monomeric IFNAR2-FCkh and IFNAR1-FChk to the SPR chip. This likely reflects the heterogeneity of the dextran/anti-FC antibody surface used to attach the proteins to the chip surface. Often, heterogeneity describes amine coupling-induced heterogeneity in the protein coupled to the matrix, which when extreme, can prevent accurate data collection and binding constants. However, in this case, we are describing positional heterogeneity of the

FC-coupled IFNAR-FCs in the dextran matrix. Specifically, all IFNAR1-FChk and IFNAR2-FCkh are coupled homogeneously on the chip surface through the FChk domain. However, within the anti-FC/dextran matrix, IFNAR1-FChk and IFNAR2-FCkh are randomly oriented in the three-dimensional space, which prevents IFNAR1 and IFNAR2 from simultaneously binding to IFNα2a. This technical issue is overcome by the IFNAR1/IFNAR2-FChk heterodimer, which allows efficient ternary complex formation. Interestingly, these heterogeneous surfaces generate off-rates equivalent to what was observed at low IFNAR1/IFNAR2 levels on supported lipid membranes.[22] These data reinforce the importance of characterizing individual cytokine–receptor interactions, as well as cytokine engagement by receptor heterodimers that more accurately reflect binding at the cell surface.

In addition to a robust reagent for characterizing protein–protein interactions, IFNAR1/IFNAR2-FChk potently antagonized IFNα2a biological activity with an IC_{50} value matching the K_D determined by SPR. Thus, the FChk domain may be a valuable scaffold for producing potent cytokine antagonists, which could have medical relevance. For example, type I IFNs have been implicated in the initiation, progression, and pathology of systemic lupus erythematosus (SLE).[29,30] Blocking type I IFN biological activity is currently being tested as a therapy for SLE and might also be important in other autoimmune diseases such as diabetes.[31–33]

Biochemical and SAXS studies confirm that FChk forms a disulfide-linked FC heterodimer that mimics the FC homodimer crystal structure. Thus, FChk forms a stable scaffold to position receptors ~20 Å apart, or further with increased linker lengths, for solution and solid-phase binding studies. Overall, our studies demonstrate that IFNAR-FChk fusion proteins are easily purified and suitable for capture on biacore chips for binding studies. These features of the system provide an opportunity for high-throughput analysis of quantitative cytokine–receptor kinetics using a standardized analysis platform. Currently, greater than 50 molecules, designated as IFNs and interleukins, are amenable to study using this strategy.[1,34,35] Preliminary studies have confirmed that FChk provides an excellent scaffold for characterizing ErbB growth factor receptor interactions[4] (K. Putcha and M.R. Walter, personal communication) and other systems are currently being evaluated.

Materials and Methods

IFNα2 expression and purification

A plasmid containing IFNα2a (*pPAL7-IFNα2a*) was obtained from Philip Bryan, which encodes a subtilisin prodomain IFNα2a fusion protein. Protein expression was performed by the autoinduction method.[36] Briefly, cells containing *pPAL7-IFNα2a* were grown at 37°C overnight with shaking (300 rpm) in ZYP 0.8G media containing 100 μg mL^{-1} carbenicillin. The overnight culture was diluted 1:20 into ZYP-5052 media and grown for 4 h at 37°C, followed by a 20-h incubation at 15°C with shaking (300 rpm). The cells were collected by centrifugation, followed by sonication in a buffer containing 100 m*M* Tris-acetate, pH 8.0 and 1.0 m*M* EDTA. The lysate was clarified by centrifugation (48,000*g*) and loaded onto eXact media (BIO-RAD). The protein was eluted with 10 m*M* sodium azide in 100 m*M* sodium acetate, pH 7.4 and subsequently purified by ion exchange and SEC. IFNα2a purified by this method retained two additional amino acids (Thr-Ser) at its N-terminus.

FChk and receptor-FChk fusion cloning, expression, and purification

DNA encoding the murine IgG2a FC region, residues 251-472 (PDB ID 1IGT), was cloned into the insect expression vector pMT (Invitrogen) by PCR. Amino acid changes E376C and T389Y were encoded into one FC sequence to generate a modified FC knob (FCk) plasmid, *pMTA-FCk*. In a second wild-type FC, a Y438T mutation was inserted and amino acids "GGCGT" were encoded at the C-terminus, following residue F472 to yield plasmid *pMTA-FCh*. The extracellular regions of IFNAR1 (residues 28-436, uniprot ID P17181) and IFNAR2 (residues 31-243, uniprot ID P48551) were inserted in frame into *pMTA-FCh* and *pMTA-FCk*, respectively, using SacII and BamHI restriction sites, resulting in plasmids *pMTA-IFNAR1-FCh* and *pMTA-IFNAR2-FC*k.

Expression plasmids were transfected into *Drosophila S2* cells using the manufacturer's protocols (Invitrogen). Stable cell lines were selected with hygromycin and protein expression was induced by addition of 0.5 m*M* Cu_2SO_4 at a cell density of 5×10^6 cells per milliliter in serum-free media (Lonza) containing 20 m*M* L-glutamine. Expressed media were harvested after 7 days, clarified by centrifugation, and filtered through a 0.2-μm PES filter. Receptor-FChk fusion proteins were purified using a 1 mL Protein A affinity column (Thermo scientific) equilibrated in 20 m*M* Tris-HCl, pH 8.0 and 150 m*M* NaCl. Bound protein was washed with 50 column volumes of equilibration buffer and eluted in 2*M* arginine, pH 3.8. The pH of the column fractions was adjusted by addition of 1*M* Tris-HCl, pH 8.0, followed by dialysis against 20 m*M* Tris-HCl, pH 8.0 and 150 m*M* NaCl. Pooled fractions were concentrated and injected on a Superdex 200 (GE Healthcare) size exclusion column in running buffer of 20 m*M* HEPES, pH 7.9 and 150 m*M* NaCl.

SPR data collection and analysis

SPR data collection and analysis were performed using a Biacore T-200 (GE healthcare). Monomeric and heterodimeric IFNAR-FChks were coupled to CM5 biacore chips using an anti-FC Ab coupling kit according to the manufacturer's instructions (GE healthcare). IFNα2a was injected over the surfaces at 100 μL min^{-1} in a running buffer of 10 m*M* HEPES, 150 m*M* NaCl, 0.015% P20 (GE Healthcare), and 150 μg mL^{-1} bovine serum albumin (Sigma). IFNα2a contact times for each experiment were 75 s. The dissociation times were 75, 240, and 400 s for IFNAR1-FChk, IFNAR2-FCkh, and IFNAR1/IFNAR2-FChk, respectively. Fresh IFNAR-FChk surfaces were prepared for each cycle by a 3-min injection of 10 m*M* glycine, pH 1.7, followed by an injection of new IFNAR-FC fusion protein. Sensorgrams were fit to appropriate 1:1 and HLMs using the predefined templates in the Biacore T-200 evaluation software version 1.0.

SAXS analysis

X-ray scattering data on FChk (8.8 mg mL^{-1}) were collected on the SIBYLS beamline at the Advanced Light Source, Berkley. Scattering curves were processed with the program PRIMUS within the ATSAS package.[37] Bead models were derived from the scattering curve with the program DAMIN.[38] A total of 10 models were calculated and a final averaged bead model was calculated with DAMAVER.

Luciferase activity assay

HT1080 cells, containing a luciferase reporter downstream of the IFN inducible 6-16 promoter (HL116 cells), were used to monitor IFNAR1/IFNAR2-FChk neutralization of IFNα2a. HL116 cells (4×10^4 cells) were plated in white opaque 96-well plates and incubated overnight at 37°C. A constant concentration of IFNα2a (8 p*M* or 5 n*M*) was incubated with serially diluted IFNAR1/IFNAR2-FChk heterodimers in media (DMEM-glutamax) for 30 min at 37°C before addition to HL116 cells. The plates were incubated for 5 h at 37°C. Following the 5-h incubation, the plates were moved to room temperature for 10 min, followed by the addition of 50 μL of luciferase assay reagent (Steady-Glo, Promega) to each well. Luminescence was measured on a Biotek Synergy 2 plate reader and analyzed with PRISM software using a four-parameter fit with variable slope (Graphpad Inc).

Acknowledgments

The authors thank Philip Bryan and Natasha Oganesyan for providing the pPal7-IFNα2a vector and expertise in protein purification, Dario Vignali for the murine IgG2a plasmid, and Gilles Uzé for HL116 cells. The SIBYLS beamline at the Advanced Light Source, Lawrence Berkeley National Laboratory, is supported in part by the DOE Program Integrated Diffraction Analysis Technologies (IDAT) under Contract Number DE-AC02-05CH11231 with the U.S. Department of Energy. Access to the Biacore T-200 is made possible by the University of Alabama at Birmingham Multidisciplinary Molecular Interaction Core.

References

1. Akdis M, Burgler S, Crameri R, Eiwegger T, Fujita H, Gomez E, Klunker S, Meyer N, O'Mahony L, Palomares O, Rhyner C, Ouaked N, Schaffartzik A, Van De Veen W, Zeller S, Zimmermann M, Akdis CA (2011) Interleukins, from 1 to 37, and interferon-gamma: receptors, functions, and roles in diseases. J Allergy Clin Immunol 127:701-721, e1-e70.
2. Commins SP, Borish L, Steinke JW (2010) Immunologic messenger molecules: cytokines, interferons, and chemokines. J Allergy Clin Immunol 125:S53-S72.
3. Bublil EM, Yarden Y (2007) The EGF receptor family: spearheading a merger of signaling and therapeutics. Curr Opin Cell Biol 19:124-134.
4. Hynes NE, Macdonald G (2009) ErbB receptors and signaling pathways in cancer. Curr Opin Cell Biol 21: 177-184.
5. LaPorte SL, Juo ZS, Vaclavikova J, Colf LA, Qi X, Heller NM, Keegan AD, Garcia KC (2008) Molecular and structural basis of cytokine receptor pleiotropy in the interleukin-4/13 system. Cell 132:259-272.
6. Thomas C, Moraga I, Levin D, Krutzik PO, Podoplelova Y, Trejo A, Lee C, Yarden G, Vleck SE, Glenn JS, Nolan GP, Piehler J, Schreiber G, Garcia KC (2011) Structural linkage between ligand discrimination and receptor activation by Type I interferons. Cell 146:621-632.
7. Logsdon NJ, Deshpande A, Harris BD, Rajashankar KR, Walter MR (2012) Structural basis for receptor sharing and activation by interleukin-20 receptor-2 (IL-20R2) binding cytokines. Proc Natl Acad Sci USA 109: 12704-12709.
8. de Vos AM, Ultsch M, Kossiakoff AA (1992) Human growth hormone and extracellular domain of its receptor: crystal structure of the complex. Science 255:306-312.
9. Wu Z, Johnson KW, Choi Y, Ciardelli TL (1995) Ligand binding analysis of soluble interleukin-2 receptor complexes by surface plasmon resonance. J Biol Chem 270: 16045-16051.
10. Chao H, Houston ME Jr, Grothe S, Kay CM, O'Connor-McCourt M, Irvin RT, Hodges RS (1996) Kinetic study on the formation of a de novo designed heterodimeric coiled-coil: use of surface plasmon resonance to monitor the association and dissociation of polypeptide chains. Biochemistry 35:12175-12185.
11. Lata S, Piehler J (2006) Synthesis of a multivalent chelator lipid for stably tethering histidine-tagged proteins onto membranes. Nat Protoc 1:2104-2109.
12. Lata S, Piehler J (2005) Stable and functional immobilization of histidine-tagged proteins via multivalent chelator headgroups on a molecular poly(ethylene glycol) brush. Anal Chem 77:1096-1105.
13. Czajkowsky DM, Hu J, Shao Z, Pleass RJ (2012) Fc-fusion proteins: new developments and future perspectives. EMBO Mol Med 4:1015-1028.
14. Ridgway JB, Presta LG, Carter P (1996) 'Knobs-into-holes' engineering of antibody CH3 domains for heavy chain heterodimerization. Protein Eng 9:617-621.

15. Borden EC, Sen GC, Uze G, Silverman RH, Ransohoff RM, Foster GR, Stark GR (2007) Interferons at age 50: past, current and future impact on biomedicine. Nat Rev Drug Discov 6:975-990.
16. Uze G, Schreiber G, Piehler J, Pellegrini S (2007) The receptor of the type I interferon family. Curr Top Microbiol Immunol 316:71-95.
17. Platanias LC (2005) Mechanisms of type-I- and type-II-interferon-mediated signalling. Nat Rev Immunol 5: 375-386.
18. Kalie E, Jaitin DA, Podoplelova Y, Piehler J, Schreiber G (2008) The stability of the ternary interferon-receptor complex rather than the affinity to the individual subunits dictates differential biological activities. J Biol Chem 283:32925-32936.
19. Jaks E, Gavutis M, Uze G, Martal J, Piehler J (2007) Differential receptor subunit affinities of type I interferons govern differential signal activation. J Mol Biol 366:525-539.
20. Cajean-Feroldi C, Nosal F, Nardeux PC, Gallet X, Guymarho J, Baychelier F, Sempe P, Tovey MG, Escary JL, Eid P (2004) Identification of residues of the IFNAR1 chain of the type I human interferon receptor critical for ligand binding and biological activity. Biochemistry 43:12498-12512.
21. Piehler J, Schreiber G (1999) Biophysical analysis of the interaction of human ifnar2 expressed in *E. coli* with IFNalpha2. J Mol Biol 289:57-67.
22. Lamken P, Lata S, Gavutis M, Piehler J (2004) Ligand-induced assembling of the type I interferon receptor on supported lipid bilayers. J Mol Biol 341:303-318.
23. Harris LJ, Larson SB, Hasel KW, McPherson A (1997) Refined structure of an intact IgG2a monoclonal antibody. Biochemistry 36:1581-1597.
24. Arndt KM, Pelletier JN, Muller KM (2002) Comparison of in vivo selection and rational design of heterodimeric coiled coils. Structure 10:1235-1248.
25. Glover JN, Harrison SC (1995) Crystal structure of the heterodimeric bZIP transcription factor c-Fos-c-Jun bound to DNA. Nature 373:257-261.
26. Manneberg M, Friedlein A, Kurth H, Lahm HW, Fountoulakis M (1994) Structural analysis and localization of the carbohydrate moieties of a soluble human interferon gamma receptor produced in baculovirus-infected insect cells. Protein Sci 3:30-38.
27. Lewerenz M, Mogensen KE, Uze G (1998) Shared receptor components but distinct complexes for alpha and beta interferons. J Mol Biol 282:585-599.
28. Lazareno S, Birdsall NJ (1993) Estimation of competitive antagonist affinity from functional inhibition curves using the Gaddum, Schild and Cheng-Prusoff equations. Br J Pharmacol 109:1110-1119.
29. Ronnblom L, Alm GV, Eloranta ML (2011) The type I interferon system in the development of lupus. Semin Immunol 23:113-121.
30. Niewold TB, Hua J, Lehman TJ, Harley JB, Crow MK (2007) High serum IFN-alpha activity is a heritable risk factor for systemic lupus erythematosus. Genes Immun 8:492-502.
31. Ronnblom L, Alm GV, Eloranta ML (2009) Type I interferon and lupus. Curr Opin Rheumatol 21:471-477.
32. Yao Y, Richman L, Higgs BW, Morehouse CA, de los Reyes M, Brohawn P, Zhang J, White B, Coyle AJ, Kiener PA, Jallal B (2009) Neutralization of interferon-alpha/beta-inducible genes and downstream effect in a phase I trial of an anti-interferon-alpha monoclonal antibody in systemic lupus erythematosus. Arthritis Rheum 60:1785-1796.
33. Diana J, Simoni Y, Furio L, Beaudoin L, Agerberth B, Barrat F, Lehuen A (2013) Crosstalk between neutrophils, B-1a cells and plasmacytoid dendritic cells initiates autoimmune diabetes. Nat Med 19:65-73.
34. Pestka S (2007) The interferons: 50 years after their discovery, there is much more to learn. J Biol Chem 282:20047-20051.
35. Kotenko SV (2011) IFN-lambdas. Curr Opin Immunol 23:583-590.
36. Studier FW (2005) Protein production by auto-induction in high density shaking cultures. Protein Expr Purif 41:207-234.
37. Konarev PV, Volkov VV, Sokolov AV, Koch MHJ, Svergun DI (2003) PRIMUS: a Windows PC-based system for small-angle scattering data analysis. J Appl Cryst 36:1277-1282.
38. Svergun DI (1999) Restoring low resolution structure of biological macromolecules from solution scattering using simulated annealing. Biophys J 76:2879-2886.